



Linear Boltzmann Equation for Solute Dispersion in Heterogeneous Media Under Non-Ergodic Conditions

Marco Dentz¹ and Arash Massoudieh²

¹Spanish National Research Council (IDAEA-CSIC), Barcelona, Spain

²Catholic University of America, Washington, DC, United States of America

Abstract

We study solute dispersion under non-ergodic conditions using a linear Boltzmann equation for the evolution of the joint distribution of the position and speed of solute particles in steady spatially heterogeneous flow fields. We show that the linear Boltzmann equation is equivalent to a time-domain random walk in which particle speeds follow a stationary spatial Markov process. It is assumed that velocity transitions can be described by stationary Gaussian copulas, which is supported by the Doob theorem. This transport framework allows to systematically study the impact of velocity correlation and non-ergodic source conditions on solute dispersion. Thus, we analyze particle transport in terms velocity statistics, displacement moments, spatial profiles and breakthrough curves for particle injections in high, intermediate and low velocity regions. We find that non-ergodic initial conditions have a significant impact on dispersion at early and intermediate times with different scaling exponents for the displacement variance than expected under ergodic conditions. They can give rise to distinctly bimodal particle distributions, and are imprinted in the peak behaviors of breakthrough curves. These results shed new light on the interpretation of dispersion data and the modeling and prediction of dispersion in heterogeneous media from the pore to the regional scales.

Keywords: Dispersion, Linear Boltzmann Equation, Heterogeneous Media, Ornstein-Uhlenbeck Process, Copulas, Markov Processes, First Passage Times

*Corresponding Author

E-mail address: marco.dentz@csic.es

doi: <https://doi.org/10.5149/ARC-GR.1401>

This work is licensed under a [Creative Commons "Attribution-NonCommercial 4.0 International"](https://creativecommons.org/licenses/by-nc/4.0/) license.



1 Introduction

Solute dispersion in geological and engineered media is determined by spatial heterogeneity in the hydraulic medium properties and in the Eulerian flow properties [11, 22, 42]. Spatial heterogeneity is present at all scales, ranging from the pore to the regional scale. At the pore scale, flow heterogeneity is induced by the complex structure of the pore space and variability in pore sizes [6]. At the continuum scale, in heterogeneous porous media, flow heterogeneity is caused by the spatial distribution of hydraulic conductivity due to the presence of different permeable materials [42]. For fractured and karst media, flow heterogeneity is due to the network structure of these media, the distribution of fracture apertures and conduit radii [4, 7]. The quantitative assessment and prediction of solute dispersion in these media is a key item in a variety of subsurface applications including groundwater contamination, underground hydrogen and carbon dioxide storage, radionuclide migration.

The impact of medium heterogeneity on solute dispersion has been quantified in terms of hydrodynamic dispersion coefficients, which integrate the effect of flow fluctuations on the spreading of a solute plume. At high Péclet numbers, the longitudinal dispersion coefficients can be quantified in terms of the average flow velocity and the characteristic heterogeneity length scale. The latter is given by the pore length on the pore scale [43], the correlation scale of hydraulic conductivity fluctuations on the continuum scale [10, 23], and the fracture or conduit lengths on the network scale. Hydrodynamic dispersion provides a framework for solute dispersion across scales, which predicts Fickian transport behaviors quantified by an advection-dispersion equation. It can explain the observation of scale effects in the dispersion of tracer plumes [24].

However, spatial variability in the hydraulic medium properties may give rise to dispersion behaviors that cannot be described by an upscaled advection-dispersion equation. Behaviors such as forward and backward tails in the spatial solute distributions and breakthrough curves as well as the non-linear evolution of the spatial moments of the distribution of solute concentration. Such deviations from Fickian behaviors have been observed at pore, continuum and regional scales, in fracture and karst networks [1, 6, 25, 30]. They can be traced back to broad distributions of solute travel times, which can be induced by broad distributions of flow velocities [16]. In heterogeneous media, velocities persist over the characteristic heterogeneity lengths scales. Thus, low velocities may persist for much longer times than high velocities, which gives rise to intermittent Lagrangian velocity series. These mechanisms can be quantified naturally in the framework of time-domain and continuous time random walks [5, 38, 39]. Furthermore, in systems with strong medium heterogeneities and velocity contrasts, the dispersion behavior depends critically on the initial solute distribution. That is, it depends on whether the solute can initially sample the full flow variability (ergodic conditions), or whether it can sample only a part of the flow spectrum (non-ergodic conditions). Dagan [12] studied the impact of non-ergodic initial distribution on longitudinal effective dispersion coefficients using perturbation theory in the velocity fluctuations. Frampton and Cvetkovic [21], Hyman et al. [29], Kang et al. [32] studied the impact of the injection mode, that is, flux or resident injection on solute transport in fracture networks.

In this paper, we analyze the impact of non-ergodic conditions on preasymptotic and asymptotic non-Fickian dispersion, which is quantified in terms of a linear Boltzmann equation for the joint distribution of position and speed of solute particles. Linear Boltzmann equations have been used for the description of solute transport in fracture media [3, 47]. Unlike upscaled advection-dispersion equations, the Boltzmann equation can be conditioned on the medium and flow heterogeneity in the source region, and thus, provides a framework for the systematic investigation of non-ergodic and non-Fickian solute transport. The evolution of Lagrangian velocities in this framework is determined by an integral term, whose

kernel is determined by the conditional probability of particle velocities, or velocity transition probability. We present the Boltzmann equation and the equivalent Lagrangian transport formulation in terms of time-domain and continuous time random walks. We discuss the representation of the velocity transition by Gaussian copula densities, and the parameterization of the model equations in terms of the Eulerian flow distribution. Then, we analyze the Lagrangian velocity statistics and solute dispersion for extreme non-ergodic initial conditions characterize by a single velocity value. We characterize intermittency of Lagrangian velocity series in terms of the increments of the normal score transforms of the particle velocities. The non-ergodic dispersion behaviors are studied in terms of spatial solute profiles and moments as well as solute breakthrough curves.

The paper is organized as follows. Section 2 introduces the linear Boltzmann equation and equivalent Lagrangian formulation, Section 2.3 discusses the transition probability of particle velocities, and Section 3 the dispersion behaviors resulting from non-ergodic conditions.

2 Linear Boltzmann Equation

We consider particle transport in heterogeneous porous media at high Péclet numbers, this means, we disregard hydrodynamic dispersion and diffusion. As particles are transported along the streamlines of a heterogeneous flow field, they change position and velocities according to the spatial flow organization. We describe the joint distribution $p(x, v, t)$ of particle position and velocity by the following linear Boltzmann equation [3, 35, 46, 47]

$$\frac{\partial p(x, v, t)}{\partial t} + \frac{v}{\chi} \frac{\partial p(x, v, t)}{\partial x} = -\frac{v}{\epsilon} p(x, v, t) + \int_0^{\infty} dv' \frac{v'}{\epsilon} p_s(v, \epsilon|v') p(x, v', t). \quad (1)$$

The left side denotes ballistic transport of the particle distribution, the right side quantifies transitions between velocities as particles move along streamlines. The first term on the right describes transitions away from the current velocity to any other velocity, the second term quantifies transitions from a velocity v' to the current velocity v . Transitions occur at variable rates that are proportional to the velocity. The transition probability is denoted by $p_s(v, \epsilon|v')$, ϵ is an intrinsic microscopic length scale over which particle velocities persist. Note that v is the particle speed, χ is advective tortuosity, and v/χ is the streamwise particle velocity. The marginal distribution $c(x, t)$ of particle positions at time t is given by

$$c(x, t) = \int_0^{\infty} dv p(x, v, t). \quad (2)$$

Analogously, the distribution of particle speeds is obtained by marginalization of $p(x, v, t)$ as

$$p(v, t) = \int_{-\infty}^{\infty} dx p(x, v, t). \quad (3)$$

Integration of (1) over x gives the evolution equation for $p(v, t)$ as

$$\frac{\partial p(v, t)}{\partial t} = -\frac{v}{\epsilon} p(v, t) + \int_0^{\infty} dv' \frac{v'}{\epsilon} p_s(v, \epsilon|v') p(v', t). \quad (4)$$

The steady state speed distribution is equal to the Eulerian speed distribution $p_e(v)$ due to volume conservation [17]. According to (4), it satisfies the equation

$$vp_e(v) = \int_0^{\infty} dv' v' p_s(v, \epsilon|v') p_e(v'). \quad (5)$$

We define now $p_s(v) = vp_e(v)/\langle v_e \rangle$, where $\langle v_e \rangle$ is the mean Eulerian speed. Thus, we can write (5) as

$$p_s(v) = \int_0^{\infty} dv' p_s(v, \epsilon|v') p_s(v'). \quad (6)$$

This means $p_s(v)$ is the eigenfunction of the transition probability $p_s(v, \epsilon|v')$ with eigenvalue 1, and is related to $p_e(v)$ through velocity weighting,

$$p_s(v) = \frac{vp_e(v)}{\langle v_e \rangle}. \quad (7)$$

2.1 Lagrangian Formulation

The Boltzmann equation (1) is equivalent to the following stochastic equations of motion of idealized solute or fluid particles

$$\frac{dx(s)}{ds} = \chi^{-1}, \quad \frac{dt(s)}{ds} = \frac{1}{v_s(s)}, \quad (8a)$$

where the particle velocities $\{v_s(s)\}$ form a Markov chain whose transition probability $p_s(v, s|v')$ satisfies the evolution equation

$$\frac{\partial p_s(v, s|v')}{\partial s} = -\frac{1}{\epsilon} p_s(v, s|v') + \frac{1}{\epsilon} \int_0^{\infty} dv'' p_s(v, \epsilon|v'') p_s(v'', s|v'), \quad (8b)$$

for the initial condition $p(v, s=0|v') = \delta(v-v')$, see also Appendix A. The variable s denotes the distance along the particle trajectory. The spatial profile is given in terms of $x(s)$ by

$$c(x, t) = \langle \delta(x - x[s(t)/\chi]) \rangle, \quad (9)$$

where $s(t) = \sup\{s|t(s) \leq t\}$. For the numerical solution of the transport equation (1) we use particle tracking based on the discretized version of the system of equations (8) as outlined in Appendix A. In Section 2.3, we discuss the representation of the transition probability $p_s(v, \epsilon|v')$ in terms of copula functions.

2.2 Continuous Time Random Walks

The system of equations (8) describes a time-domain random walk (TDRW) because the time increments $dt = ds/v_s(s)$ are correlated random variables. Their evolution is described by the spatial Markov processes for the particle velocities (8b) whose transition probability satisfies the Chapman-Kolmogorov equation. For space increments ℓ_0 larger than the correlation length ℓ_c , subsequent velocities are independent and (8) can be coarse-grained as

$$x_{n+1} = x_n + \ell_0 \quad t_{n+1} = t_n + \tau_n, \quad \tau_n = \frac{\ell_0}{v_n}, \quad (10a)$$

where the scale $\ell_0 \geq \ell_c$ depends on the properties of the transition probability $p_s(v, s|v')$. The velocities v_n are independent identically distributed random variables characterized by the distribution $p_s(v)$, such that the time increment τ_n is distributed according to

$$\psi(t) = \frac{\ell_0}{t^2} p_s(\ell_0/t). \quad (10b)$$

Equations (10) describe a continuous time random walk (CTRW). This allows us to use well-known results from the CTRW framework to assess the asymptotic transport behaviors, that is, for long times and travel distances.

2.3 Transition Probability of Particle Velocities

The transition probability $p_s(v, s|v')$ lies at the heart of the Boltzmann approach to particle motion in heterogeneous flow fields. Here we briefly discuss the analysis and modeling of $p_s(v, s|v')$. To this end, we recall the kinematic equation that describes particle motion in a steady heterogeneous flow field (\mathbf{x}),

$$\frac{d\mathbf{x}(t)}{dt} = \boldsymbol{\ell}(t), \quad (11)$$

where $\boldsymbol{\ell}(t) = [\mathbf{x}(t)]$ is the isochrone Lagrangian velocity. The travel distance $s(t)$ and the travel time $t(s)$ along a particle paths are

$$\frac{ds(t)}{dt} = v_\ell(t), \quad \frac{dt(s)}{ds} = \frac{1}{v_\ell[t(s)]} \equiv \frac{1}{v_s(s)}. \quad (12)$$

where $v_\ell(t) = |\boldsymbol{\ell}(t)|$. The equidistant Lagrangian speed $v_s(s)$ is obtained by sampling the speed $v_\ell(t)$ at times $t(s)$ that correspond to streamline distances s . Thus, the series $\{v_s(s)\}$ of Lagrangian speeds are obtained through equidistant sampling along particle trajectories [17, 26, 41]. The transition probability from $v' = v_s(s)$ to $v = v_s(s + \Delta s)$ is defined by

$$p_s(v, \Delta s|v') = \frac{p_s(v, v', \Delta s)}{p_s(v')}, \quad (13)$$

where we assume that the velocity series is stationary, that is, its statistics depends only on the space increment Δs . The joint distribution of $v(s + \Delta s)$ and $v(s)$ is defined by sampling along trajectories as

$$p_s(v, v', \Delta s) = \langle \delta[v - v(s + \Delta s)] \delta[v' - v(s)] \rangle, \quad (14)$$

where the angular brackets denotes the average over all particles and $\delta(\cdot)$ denotes the Dirac delta. The one-point distribution is defined by

$$p_s(v) = \langle \delta[v - v(s)] \rangle. \quad (15)$$

Many stochastic Markov models [31, 33, 44] for the quantification of dispersion in heterogeneous media employ empirical transition probabilities. One can obtain further insight into the nature of the velocity transitions by considering the copula of the velocity series.

Copula functions characterize the correlation properties of the velocity series $\{v_s(s)\}$ without bias from the marginal distribution $p_s(v)$ and thus provide an objective basis for the modeling of the velocity transition probability. The transition probability or conditional probability $p_s(v, s|v')$ can be written in terms of the copula density $\theta(u, u')$ as [37]

$$p_s(v, s|v') = p_s(v) \theta[p_s(v), p_s(v')], \quad (16)$$

see Appendix B for further details. The copula function can be seen as the transition probability between equiprobable velocity bins. To see this, we define the velocity ranks $u(s) \in [0, 1]$ as

$$u(s) = P_s[v(s)], \quad P_s(v) = \int_0^v dv' p_s(v'). \quad (17)$$

Thus, the copula density can be obtained by jointly sampling $u(s)$ and $u(s')$ along particle trajectories,

$$\theta(u, u') = \langle \delta[u - u(s)] \delta[u' - u(s')] \rangle. \quad (18)$$

By definition, the marginal distributions of u and u' are uniform, and thus, the joint distribution $\theta(u, u')$ is identical to the conditional distribution, or transition probability. Thus, the intervals or bins $[u, u + du]$ are equiprobable and so are the corresponding velocity intervals. Therefore, $\theta(u, u') du$ denotes the transition probability between equiprobable velocity intervals.

We focus in the following on the Gaussian copula density [37]

$$\theta_G(u, u', r) = \frac{\exp\left[\frac{\Phi^{-1}(u)^2 r^2 - 2r\Phi^{-1}(u)\Phi^{-1}(u') + \Phi^{-1}(u')^2 r^2}{2(1-r^2)}\right]}{\sqrt{1-r^2}}, \quad (19)$$

where r denotes the correlation coefficient. The cumulative Gaussian distribution $\Phi(w)$ and its inverse $\Phi^{-1}(u)$ are given by

$$\Phi(w) = \frac{1}{2} \left[1 + \operatorname{erf}(w/\sqrt{2}) \right], \quad \Phi^{-1}(u) = \sqrt{2} \operatorname{inverf}(2u - 1), \quad (20)$$

where $\operatorname{inverf}(u)$ is the inverse error function. The transition probability $p_s(v, s|v')$ reads in terms of the Gaussian copula as

$$p_s(v, s|v') = p_s(v) \theta_G[P_s(v), P_s(v'), \mathcal{C}(s)]. \quad (21)$$

Note that the correlation coefficient $r \equiv \mathcal{C}(s)$ in general depends on the distance s between the sampling points.

The statement that the velocity series $\{v_s(s)\}$ has a Gaussian copula, is equivalent to the statement that the normal score transform of $\{v_s(s)\}$ describes an Ornstein-Uhlenbeck process, under the condition that $\mathcal{C}(s) = \exp(-s/\ell_c)$, where ℓ_c is the correlation length scale. This proposition is shown in Appendix C by using the Doob theorem [19]. The normal score transform of $v_s(s)$ is defined by

$$w_s(s) = \Phi^{-1}(P_s[v_s(s)]). \quad (22)$$

Thus, if $v_s(s)$ has a Gaussian copula with an exponential correlation function, $w_s(s)$ describes the Ornstein-Uhlenbeck process

$$\frac{dw_s(s)}{ds} = \ell_c^{-1} w_s(s) + \sqrt{2\ell_c^{-1}} \xi(s), \quad (23)$$

where $\xi(s)$ denotes a Gaussian white noise with zero mean and correlation function $\langle \xi(s)\xi(s') \rangle = \delta(s - s')$. The Ornstein-Uhlenbeck process has been shown to describe particle motion and velocity transitions at the pore [36, 40], Darcy [8] and fracture network scales [15, 28]. Thus, this indicates that the process $\{v_s(s)\}$ can indeed be characterized by a Gaussian copula for a range of scales in porous and fractured media. Thus, in the following, we will use the Gaussian copula, or equivalently, the Ornstein-Uhlenbeck process for the normal score of $v_s(s)$ in order to explore the impact of non-ergodic conditions on particle dispersion in heterogeneous flow fields.

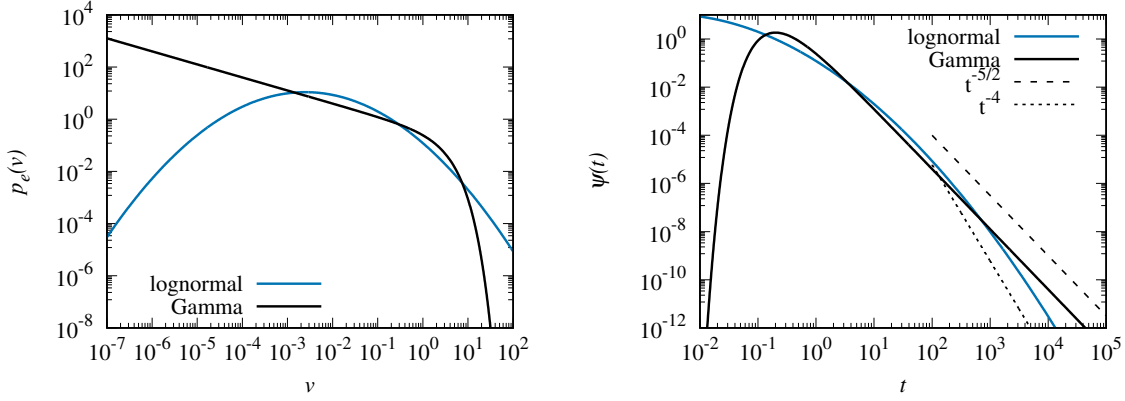


Figure 1: The left panel shows the (blue) Lognormal distribution with $\sigma_f^2 = 4$ and (black) Gamma distribution with $\alpha = 1/2$ for $\langle v_e \rangle = 1$. The right panel shows the corresponding transition time distributions $\psi(t)$.

3 Non-Ergodic Dispersion Behaviors

The Boltzmann equation (1) provides a model for solute and particle transport in across scales in heterogeneous media that can be conditioned on the initial velocity data, that is, it can be conditioned on the injection location if information on the permeability distribution of flow velocities is available. In the following, we highlight transport features that emerge from non-stationary initial conditions, that is, from initial conditions that are far from equilibrium. With equilibrium condition we mean an initial distribution that is equal to the steady state velocity distribution, which is the Eulerian distribution $p_e(v)$ for velocity sampling in space and the flux-weighted Eulerian distribution $p_s(v)$ for sampling in time.

As models for the Eulerian velocity distribution $p_e(v)$, we consider here the lognormal and Gamma distributions

$$p_e(v) = \frac{\exp\left(-[\ln(v) - \mu]^2 / 2\sigma_f^2\right)}{v\sqrt{2\pi\sigma_f^2}}, \quad (24)$$

$$p_e(v) = \frac{1}{v_0\Gamma(\alpha)} \left(\frac{v}{v_0}\right)^{\alpha-1} \exp[-(v/v_0)]. \quad (25)$$

The lognormal distribution, and power-law distributions of the type of the Gamma distribution have been found to represent the variability of hydraulic conductivity in heterogeneous porous media at pore and continuum scale [2, 9, 14, 18, 20]. The Lagrangian speed distribution $p_s(v)$ is related to the Eulerian distribution $p_e(v)$ by (7). In order to compare the transport behaviors for the two speed distributions, we consider the same mean speeds. The mean Eulerian speed for the lognormal and Gamma distributions are

$$\langle v_e \rangle = \exp(\mu + \sigma_f^2/2), \quad \langle v_e \rangle = \alpha v_0. \quad (26)$$

respectively. We set in the following $\langle v \rangle = 1$. Furthermore, for the computational examples discussed in the following, we set $\sigma_f^2 = 4$ and $\alpha = 0.5$ as illustrated in Figure 1 along with the corresponding transition time distributions $\psi(t)$ defined by Eq. (10b). As non-ergodic initial conditions, we consider the deterministic

$$p_0(v) = \delta(v - v_0). \quad (27)$$

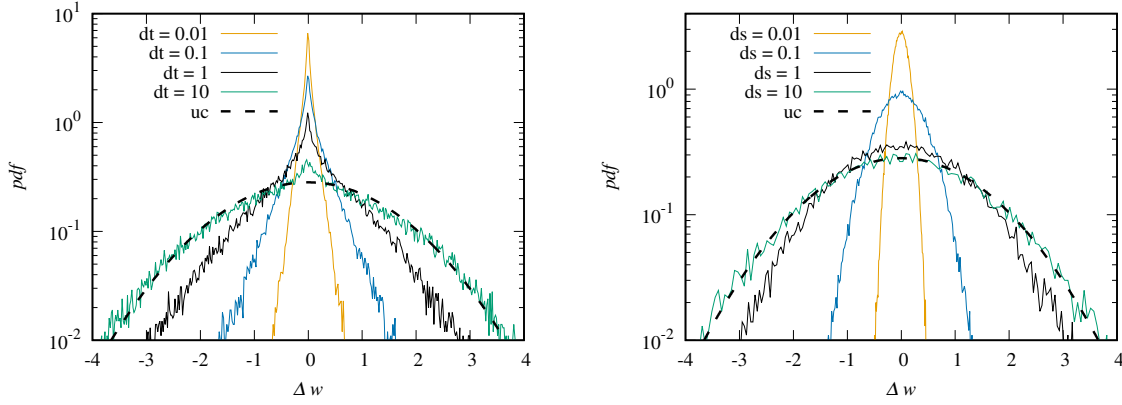


Figure 2: Distribution of increments of the normal score transform of the particle velocities (left) for different time lags and (right) for different space lags along trajectories for Gamma-distributed velocities with $\alpha = 1/2$ and $\langle v_e \rangle = 1$. The dashed lines indicated the increment distribution for uncorrelated normal scores.

This extreme initial condition corresponds to tracer injection into a region characterized by the velocity v_0 , and serves to illustrate the impact of non-ergodic injection conditions on solute dispersion. The behaviors for these initial conditions are contrasted with the ones for ergodic initial conditions. As outlined in Section 2, $p(v, t)$ evolves toward the stationary limit $p_e(v)$, the Eulerian velocity distribution. The distribution $p_s(v, t)$ of particle velocities in space evolves toward the stationary distribution $p_s(v)$. Thus, in the following, we employ the ergodic initial condition

$$p_0(v) = p_e(v), \quad (28)$$

when we consider displacement statistics. When we consider breakthrough curves, that is, arrival time distribution measured at fixed positions in space, the ergodic initial condition is the flux-weighted Eulerian distribution,

$$p_0(v) = p_s(v). \quad (29)$$

We solve the Boltzmann transport equation (1) using the random walk particle tracking algorithm detailed in the previous section and in Appendix A. The correlation length is set to $\ell_c = 1$. We first discuss the Lagrangian velocity statistics as a function of time and distance along streamlines. Then we analyze the impact of non-ergodic initial conditions on spatial concentration profiles, the displacement mean and variance, and solute breakthrough curves.

3.1 Lagrangian Velocity Statistics

We discuss here two aspects of Lagrangian velocity statistics in order to highlight the impact of correlation in time and space on Lagrangian velocity series, and the impact of non-ergodic initial conditions and their persistence in time and space. For the first item, we consider distributions of the increments of the normal score transforms of the particle velocities $v_t(t)$ and $v_s(t)$ at different lag times and lag distances. For the second item, we consider the evolution of the conditional mean velocities in time and space.

3.1.1 Distribution of Normal Score Increments

We discuss here the correlation and intermittent character of Lagrangian velocity series. The distribution of velocity increments is an indicator for intermittency and persistence of particle

velocities [13, 27, 36]. For the dynamics described by the Boltzmann equation and equivalent Lagrangian framework, small velocities are more persistent than large transport velocities because the persistence time is equal to the characteristic length scale ℓ_c divided by the current velocity $v_s(s)$. This behavior manifests in a peak at zero because the strong correlation of subsequent velocities implies a small value for the velocity increment. For the velocity fields under consideration here, this is not practical because the increment statistics even for uncorrelated velocities show a peak at zero due to the relative high probability of small velocities. Thus, in order not obscure the peak behavior due to correlation, we consider the normal scores of the particle velocities $v_t(t)$ sampled in time and $v_s(s)$ in space. The normal score transform $w_s(s)$ of $v_s(s)$ is defined by Eq. (22). The normal score transform of $v_t(t)$ is defined analogously by

$$w_t(t) = \Phi^{-1}(p_s[v_t(t)]). \quad (30)$$

The single point distributions of $w_s(s)$ and $w_t(t)$ are by definition given by unit the Gaussian distribution. The increments of the normal scores are defined by

$$\Delta w_t(t, \Delta t) = w_t(t + \Delta t) - w_t(t), \quad \Delta w_s(s, \Delta s) = w_s(s + \Delta s) - w_s(s), \quad (31)$$

with the lag distances in time and space denoted by Δs and Δt . We consider velocity series under statistically stationary conditions. That is, the distribution of initial velocities v_0 is equal to the Eulerian velocity PDF $p_e(v)$ for temporal sampling and for spatial sampling it is given by $p_s(v)$. The increment distribution for uncorrelated normal scores is given by

$$p_{\Delta w} = \frac{\exp\left(-\frac{w^2}{4}\right)}{2\sqrt{\pi}}. \quad (32)$$

Figure 2 shows the distribution of normal score increments for Gamma-distributed velocities. For lognormal velocities the behavior is qualitatively very similar and not shown here. The distributions of $\Delta w_t(t, \Delta t)$ are peaked at zero, which indicates the strong velocity correlation in time, specifically of small velocities as outlined above. The distributions widen with increasing time lag, but the peak at zero persists even for large Δt . While the tails of the distribution converge toward Eq. (32), the peak persists. This is different for the increment distributions sampled in space. There, the increment distributions are represented by narrow Gaussians, whose widths increase with increasing lag distance. The distributions converge to the limit distribution (32) for $\Delta s > \ell_c$.

3.1.2 Mean Velocity

We consider the relaxation of the mean transport velocity from a fixed initial value v_0 in space and time toward the respective steady state values $\langle v_s \rangle$ and $\langle v_e \rangle$. They evolve according to

$$\langle v_s | v_0 \rangle = \int_0^\infty dv p_s(v, s | v_0), \quad \langle v_t | v_0 \rangle = \int_0^\infty dv p_t(v, t | v_0). \quad (33)$$

In the case of a lognormal speed distribution, we obtain for $\langle v_s | v_0 \rangle$ the explicit expression

$$\langle v_s | v_0 \rangle = \langle v_s \rangle \exp \left[(\ln v_0 - \mu) \exp(-\gamma s) - \frac{\sigma_f^2 \exp(-2\gamma s)}{2} \right], \quad (34)$$

Figure 3 shows the evolution of the mean velocity for different out-of-equilibrium initial conditions in time and with distance. The evolution of $\langle v_t | v_0 \rangle$ is determined by the initial

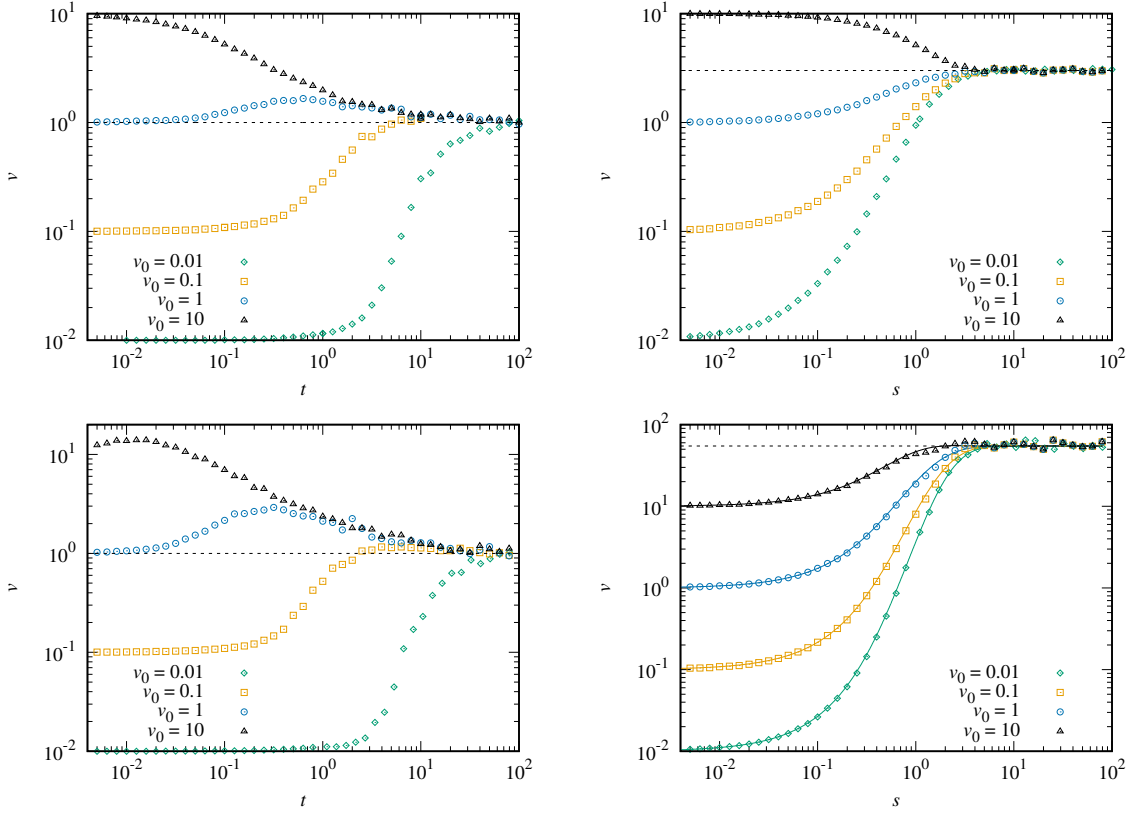


Figure 3: Mean velocities for the (top) Gamma distribution and (bottom) lognormal velocity distribution. The left column shows the evolution in time, the right with distance along streamlines. The dashed lines indicate the respective asymptotic mean velocities. The solid lines in the bottom right figure denote the analytical expression (34). The dashed lines denote the respective asymptotic mean velocities.

velocity v_0 because the evolution time scale is given by ℓ_c/v_0 . For $v_0 = \langle v_e \rangle$, the velocity first evolves to larger values before it converges back toward $\langle v_e \rangle$. Note that even though $v_0 = \langle v_e \rangle$ is equal to asymptotic mean velocity does not imply that the system is in equilibrium. The spatial evolution of the mean velocity $\langle v_s | v_0 \rangle$ toward to the asymptotic $\langle v_s \rangle$ is determined only by the correlation length ℓ_c and is not affected by the initial velocity.

3.2 Displacement Statistics

Figure 4 shows spatial concentration profiles $c(x, t)$ at different times t for the initial velocities $v_0 = 0.1, 1, 10$ and for ergodic initial conditions. For the ergodic initial condition, we observe strong retention in the source region due to sampling from the low flow velocities in the initial distribution, and a forward peak due to particles with initial velocities higher than the mean. For $v_0 = 0.1$, we observe the formation of a slowly moving peak due to the persistence of the low injection velocity and the formation of a forward peak due to particle transitions toward higher velocities. For increasing v_0 , the bulk of the particles is transported at high flow speeds, which manifests in a leading edge and the formation of a trailing tail due to particles that transition to low velocities. Such features have been observed both in laboratory and field experiments [1, 34].

Figure 5 shows the corresponding displacement mean and variance for the Gamma and

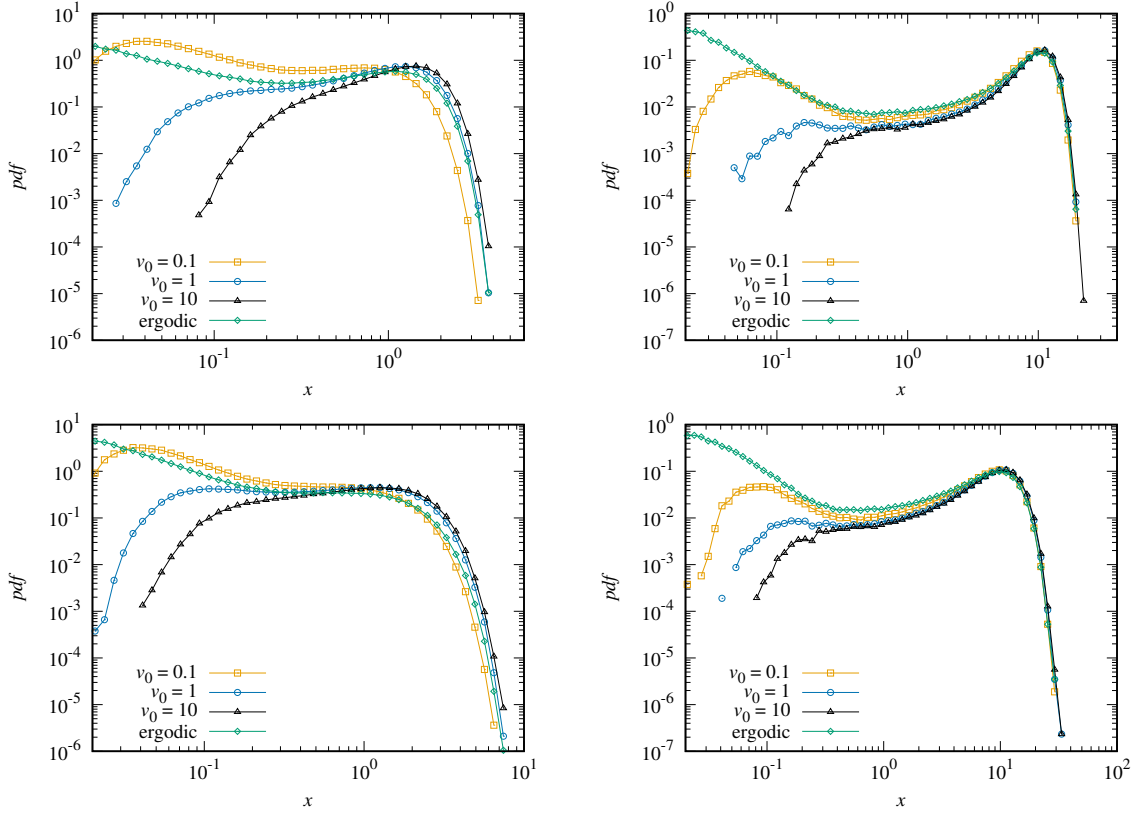


Figure 4: Spatial concentration profiles for the (top) Gamma distribution and (bottom) lognormal velocity distribution for (left) $t = 1$ and (right) $t = 10$ for the initial velocities $v_0 = 0.1, 1, 10$.

lognormal velocity distributions. Displacement mean and variance are defined by

$$m(t) = \langle x(t) \rangle, \quad \kappa(t) = \langle x(t)^2 \rangle - \langle x(t) \rangle^2. \quad (35)$$

The mean displacements evolve first with the initial velocity v_0 and then converge to the asymptotic behavior characterized by $\langle v_e \rangle$. The time of convergence depends on the initial velocity as discussed also in the context of the mean particle velocities in Section 3.1. For the ergodic initial condition, the mean displacement evolves linearly in time as $m(t) = \langle v_e \rangle t$. The displacement variances increase at short times as $\kappa(t) \propto t^3$ in contrast to the behavior for an ergodic source, for which we observe ballistic growth as $\kappa \propto t^2$, see Appendix D. For the Gamma distributed velocities, the $\kappa(t)$ then cross over towards the asymptotic scaling $t^{2-\alpha}$, which is obtained from CTRW theory [5, 45]. It is independent from the initial velocity distribution. For the lognormal velocity distribution, dispersion is asymptotically Fickian, that is, $\kappa(t)$ asymptotically scales linearly with time. Due to the broad distribution of particle velocities, this asymptotic regime is reached only after a long cross-over that itself can be characterized by power-law tangents as indicated in Figure 5.

3.3 Breakthrough Curves

The breakthrough time $t(s)$ at a distance $x = s/\chi$ from the inlet is a random variable according to Equation (8). The breakthrough curve is determined as the distribution of breakthrough times

$$f(t, x) = \langle \delta [t - t(x\chi)] \rangle. \quad (36)$$

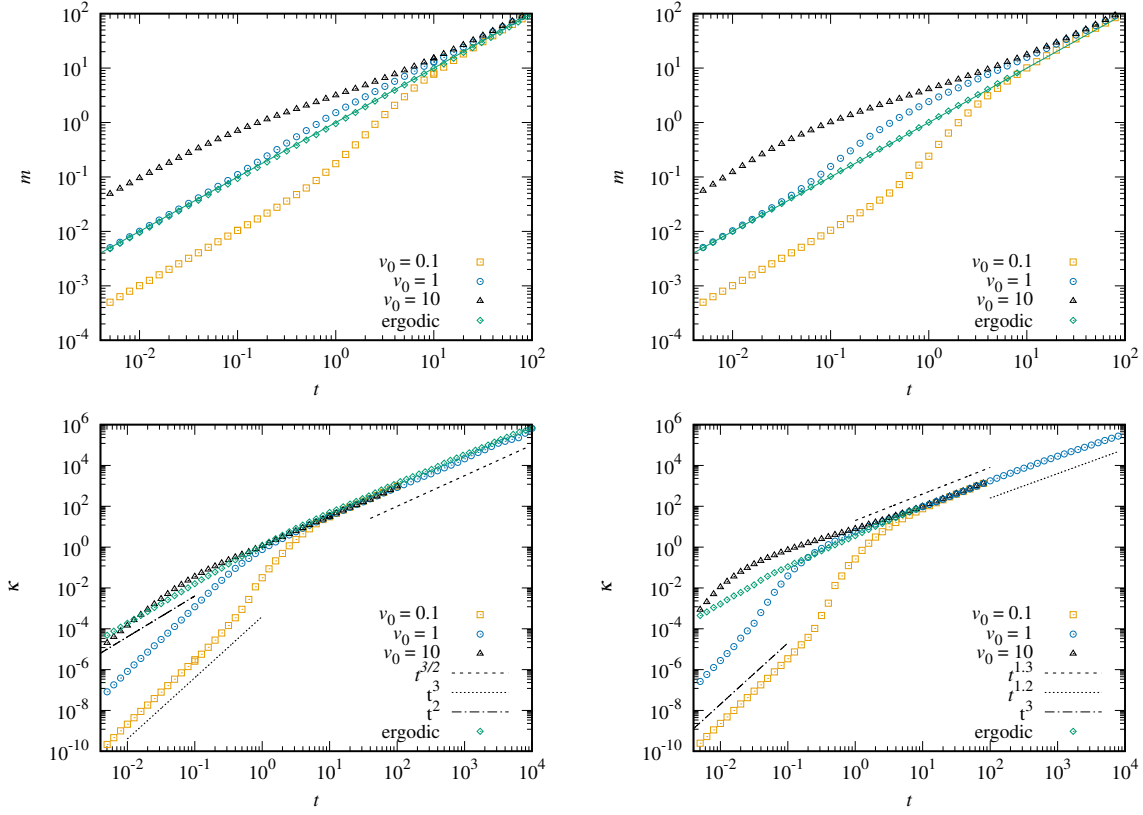


Figure 5: The top row shows the mean displacement for (left) Gamma and (right) lognormally distributed velocities. The bottom row shows the corresponding displacement variance. The initial velocities are $v_0 = 0.1, 1, 10$.

Figure 6 shows breakthrough curves for the lognormal and Gamma velocity distributions at distances $x = \ell_c$ and $10\ell_c$ from the inlet for non-ergodic and ergodic initial conditions. Note that the ergodic initial condition is here $p_0(v) = p_s(v)$. At $x = \ell_c$, the peak arrival times decrease with increasing initial velocities v_0 , while the tailing behaviors are similar for all breakthrough curves. For the Gamma distributed velocities, the tail behavior is determined by the characteristic power-law $f(t, x) \propto t^{-2-\alpha}$ which can be obtained from CTRW theory [5] according to Section 2.2. For the lognormal velocity distribution, the tail behavior does not follow a clear power law. For $x = 10\ell_c$ it can be characterized by a power-law tangent that scales as t^{-4} . This scaling can be traced back to a corresponding power-law tangent in the transition time distribution $\psi(t)$ as shown in Figure 1. With increasing distance, the difference in the peak arrivals has decreases as particles sample more flow speeds away from the initial velocities. The breakthrough curves converge towards the ergodic breakthrough curves irrespective of the initial velocity, or in other words, the (spatial) memory of the initial velocity vanishes.

4 Conclusions

We study solute dispersion in heterogeneous media under non-ergodic conditions as described by a linear Boltzmann equation for the joint distribution of particle positions and velocities. The equivalent Lagrangian transport equations are shown to describe a time-domain random walk, where particle velocities follow a stationary spatial Markov process. Using a Gaussian copula for the velocity transitions, this transport framework is parameterized by a character-

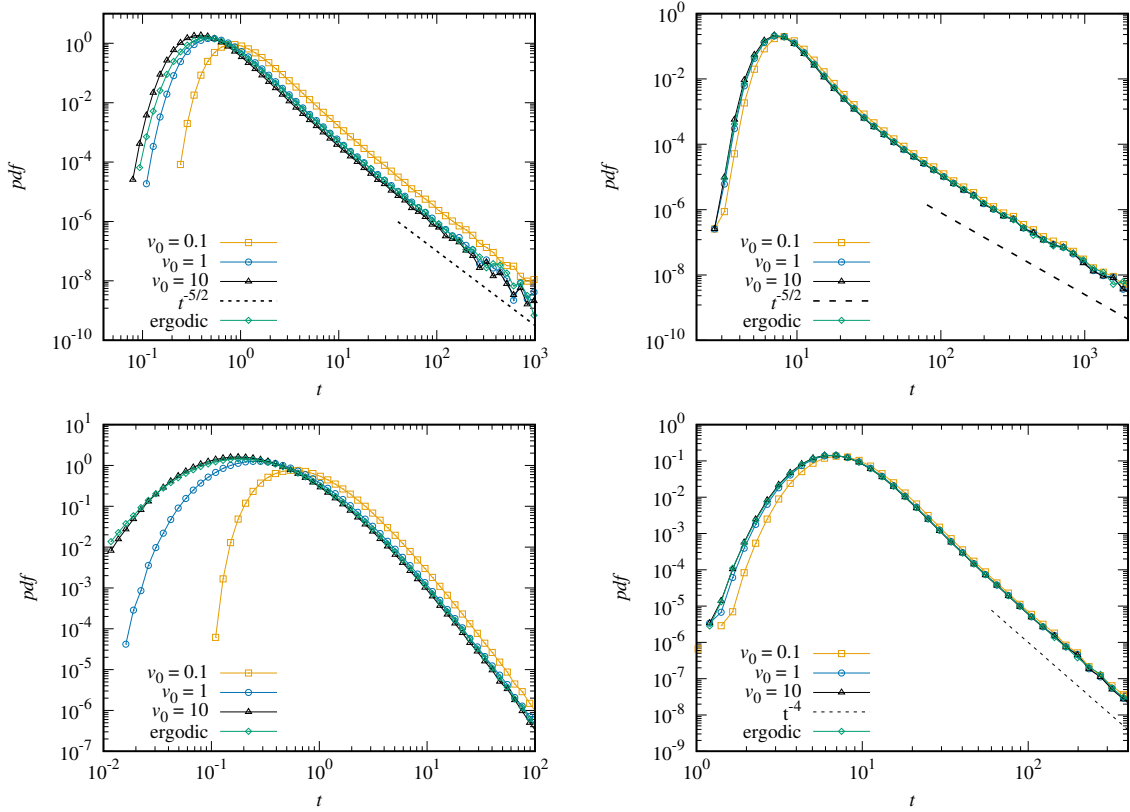


Figure 6: Breakthrough curves for (top) Gamma distributed and (bottom) lognormally distributed velocities for distances of (left) $x = 1$ and (right) $x = 10$ from the inlet, for $v_0/\langle v_e \rangle = 0.1, 1, 10$ and for $p_0(v) = p_s(v)$.

istic correlation length and the steady state speed distribution. This approach is valid across scales in heterogeneous media for which particle velocities evolve on characteristic medium length scales. That is, it is valid for pore, continuum and network scale flow and transport, and can be conditioned on the velocity distribution in the source zone. Thus, it allows to systematically analyze the impact of velocity correlation and non-ergodic source conditions on solute dispersion.

The spatial persistence of particle velocities over the correlation scale implies that small particle velocities persist over much longer times than high velocities. Therefore, temporal velocity series are characterized by intermittent patterns, that is, long periods of small velocities and periods of rapid velocity changes. We analyze the intermittency of Lagrangian velocity series in terms of increment distributions. Intermittency is characterized by a distinct peak at the origin of the increment distribution, which is caused by the spatial persistence of particle velocities. Due to the non-Gaussian nature of velocity distributions in heterogeneous media, the distribution of velocity increments are not well-suited to discuss this aspect because they are typically skewed towards small values. Thus, we propose to quantify intermittency by the distributions of increments of the normal scores of the particle velocities, which have by definition a unit Gaussian distribution. Increment distributions sampled in time show a distinctly intermittent behavior characterized by persistent peaks at the origin due to the strong temporal persistence of low velocities. This intermittency is removed for the space-sampled increments. The spatial and temporal persistence of initial particle velocities have a significant impact on the preasymptotic dispersion behavior. We analyze particle transport for source conditions characterized by particle injection into low intermediate and high velocity

channels. For low initial velocities, the spatial solute distribution can develop double peak behaviors. At early times, the displacement variance increase with the third power of time as opposed to ballistic scaling with the square of time, what is expected for ergodic conditions. For the breakthrough curves a notable difference between the injections modes can only be observed at distances close to the inlet plane.

These findings can shed light on the interpretation of dispersion data in heterogeneous media measured at the field or laboratory scale, and on their relation to the source conditions and velocity correlations. They can guide the analysis of Lagrangian velocity series obtained for example from particle tracking velocimetry in laboratory experiments and direct numerical simulations, and the identification and classification of non-Fickian and anomalous dispersion behaviors at pore, continuum and network scales.

Acknowledgements

M.D. acknowledges funding by the European Union (ERC, KARST, 101071836). Views and opinions expressed are, however, those of the authors only, and do not necessarily reflect those of the European Union or the European Research Council Executive Agency. Neither the European Union nor the granting authority can be held responsible for them.

Data Availability

The data and scripts to generate the figures in this work are available at <http://hdl.handle.net/10261/382798>.

Author Contributions

MD: Conceptualization, Methodology, Software, Writing—Original Draft, Writing—Review and Editing, Visualization, Funding Acquisition.

AM: Conceptualization, Methodology, Writing—Review and Editing.

A Lagrangian Equations of Motion and Particle Tracking

The discretized version of (8) is given by

$$x(s + ds) = x(s) + ds/\chi, \quad t(s + ds) = t(s) + ds/v(s). \quad (37)$$

In order to derive the transition probability from $v(s) = v'$ to $v(s + ds) = v$, we consider (8b) for a lag distance $ds \leq \epsilon$ and expand up to linear order in ds . This gives

$$p_s(v, ds|v') = \delta(v - v') \left(1 - \frac{ds}{\epsilon} \right) + \frac{ds}{\epsilon} p_s(v, \epsilon|v'), \quad (38)$$

where we used that $p_s(v, s = 0|v') = \delta(v - v')$.

With this preparation, we show now the equivalence between the Lagrangian formulation (8) and the Eulerian evolution equation (1). Thus, we note that the joint distribution $p(x, v, t)$ is defined by

$$p(x, v, t) = \langle \delta[x - s/\chi] \delta[v - v[s(t)]] \rangle, \quad (39)$$

where $s(t) = \min[s|t(s) \leq t]$. We can write this equation as

$$p(x, v, t) = \int_0^\infty ds \langle \delta[x - s/\chi] \delta[v - v(s)] \delta[s - s(t)] \rangle. \quad (40)$$

The latter can be written as

$$p(x, v, t) = v^{-1} \int_0^\infty ds R(x, v, t, s), \quad (41)$$

where we defined

$$R(x, v, t, s) = \langle \delta[x - s/\chi] \delta[v - v(s)] \delta[t - t(s)] \rangle \quad (42)$$

The latter is the density of the Markov process $\{x(s), v(s), t(s)\}$ and satisfies the Kolmogorov equation

$$R(x, v, t, s + ds) = \int_0^t dt' \int_0^\infty dx' \int_0^\infty dv' R(x - ds/\chi, v', t - ds/v') p_s(v, ds|v'). \quad (43)$$

Using expression (38) and considering the limit of $ds \rightarrow 0$, we obtain

$$\begin{aligned} R(x, v, t, s + ds) &= R(x, v, t, s) - \frac{ds}{\chi} \frac{\partial R(x, v, t, s)}{\partial x} - \frac{ds}{v} \frac{\partial R(x, v, t, s)}{\partial t} \\ &\quad - \frac{ds}{\epsilon} R(x, v, t, s) + \frac{ds}{\epsilon} \int_0^\infty dv' R(x, v', t) p_s(v, \epsilon|v') + \dots, \end{aligned} \quad (44)$$

where the dots denote contributions of order ds^2 . Thus, we obtain in the limit $ds \rightarrow 0$

$$\begin{aligned} \frac{\partial R(x, v, t, s)}{\partial s} + \frac{1}{v} \frac{\partial R(x, v, t, s)}{\partial t} + \frac{1}{\chi} \frac{\partial R(x, v, t, s)}{\partial x} \\ - \frac{1}{\epsilon} R(x, v, t, s) + \frac{1}{\epsilon} \int_0^\infty dv' R(x, v', t) p_s(v, \epsilon|v'). \end{aligned} \quad (45)$$

Using that

$$\int_0^\infty ds R(x, v, t, s) = vp(x, v, t) \quad (46)$$

according to (41), we obtain (1). This shows the equivalence between the Lagrangian framework given by (8) and the Eulerian framework given by (1).

The particle tracking simulations are based on the discrete equations

$$x(s + \Delta s) = x(s) + \Delta s/\chi, \quad t(s + \Delta s) = t(s) + \Delta s/v(s). \quad (47)$$

We choose $\epsilon \ll \Delta s \ll \ell_c$. At each step, particles are displaced by the space increment $\Delta s/\chi$ and time increment $\Delta s/v(s)$, while the velocity $v(s)$ is drawn from the conditional probability density $p_s(v, \Delta s|v')$.

B Copulas

Here we briefly summarize the copula method for the representation of joint and conditional probabilities. To this end, we consider the joint distribution

$$p_s(v, v', \Delta s) = p_s(v, \Delta s|v')p_s(v'), \quad (48)$$

The respective cumulative distributions are defined by

$$P_s(v, v', \Delta s) = \int_0^v dv_1 \int_0^{v'} dv_2 p_s(v_1, v_2, \Delta s), \quad P_s(v) = \int_0^v dv' p_s(v') \quad (49)$$

The cumulative joint distribution $P_s(v, v', \Delta s)$ can be expressed as [37]

$$P_s(v, v', \Delta s) = \Theta[P_s(v), P_s(v')] \quad (50)$$

where $\Theta(u, u')$ is a copula function. We consider here two-dimensional copula functions. A Copula function is any monotonically increasing function with respect to its arguments mapping from $[0, 1]^2 \rightarrow [0, 1]$ with the properties

$$\Theta(u, 0) = \Theta(0, u') = 0, \quad \Theta(1, u') = u', \quad \Theta(u, 1) = u. \quad (51)$$

Taking the derivative of (50) with respect to v and v' the joint probability distribution of v and v' is

$$p_s(v, v', \Delta s) = p_s(v)\theta[P_s(v), P_s(v')]p_s(v'), \quad (52)$$

where θ is the copula density function

$$\theta(u, u') = \frac{\partial^2 \Theta(u, u')}{\partial u \partial u'}. \quad (53)$$

It is the joint density of u and u' . The transition probability or conditional probability of $p(v|v')$ is obtained from (52) according to Bayes theorem as

$$p(v, \Delta s|v') = p_s(v)\theta[P_s(v), P_s(v')]. \quad (54)$$

C Gaussian Copulas and the Ornstein-Uhlenbeck Process

According to the Doob theorem [19] any process that is Markovian, stationary and Gaussian is an Ornstein-Uhlenbeck process. The process $\{w_s(s)\}$ has a Gaussian distribution by definition, that is, $\phi(w)$ is a unit Gaussian. Thus, the conditional distribution can be directly obtained by variable transform from Eq. (21) by noting that $P_s[v_s(s)] = \Phi[w_s(s)]$. This gives

$$\phi(w, s|w') = \frac{\exp\left(-\frac{[w-w'\mathcal{C}(s)]^2}{2[1-\mathcal{C}(s)^2]}\right)}{\sqrt{2\pi[1-\mathcal{C}(s)^2]}}. \quad (55)$$

For $w_s(s)$ to be a stationary Markov process, its conditional probability $\phi(w, s|w')$ needs to fulfill the Chapman-Kolmogorov equation, that is,

$$\phi(w, s + \Delta s|w') = \int_{-\infty}^{\infty} dw'' \phi(w, \Delta s|w'')\phi(w'', s|w'). \quad (56)$$

Using (55) on the right side gives

$$\phi(w, s + \Delta s | w') = \frac{\exp \left[-\frac{w^2 + w'^2 \mathcal{C}(s)^2 \mathcal{C}(\Delta s) - 2\mathcal{C}(s)\mathcal{C}(\Delta s)ww'}{2[1 - \mathcal{C}(s)^2 \mathcal{C}(\Delta s)^2]} \right]}{\sqrt{2\pi[1 - \mathcal{C}(s)^2 \mathcal{C}(\Delta s)^2]}} \quad (57)$$

Thus, for the Chapman-Kolmogorov equation to hold $\mathcal{C}(s)$ needs to satisfy

$$\mathcal{C}(s + \Delta s) = \mathcal{C}(\Delta s)\mathcal{C}(s). \quad (58)$$

D Early Time Scaling of Displacement Variance

In this section, we derive the cubic early time scaling of the displacement variance for a non-ergodic source with fixed velocity v_0 and for an ergodic source, for which the initial velocities are distributed according to $p_e(v)$. To this end, we note first that the particle speed $v_s(s)$ can be written in terms of the normal score $w_s(s)$ as

$$v_s(s) = F[w_s(s)] = p_s^{-1}(\phi[w_s(s)]). \quad (59)$$

Then, we consider Eq. (23) for $w(s)$. For small displacements $s \ll 1/\gamma$, we can write

$$w(s) = w_0 + \zeta(s), \quad \zeta(s) = \sqrt{2\gamma} \int_0^s ds' \xi(s'). \quad (60)$$

Thus, the particle velocity can be approximated by

$$v_s(s) = F[w_0 + \zeta(s)] = F(w_0) + \frac{dF(w_0)}{dw} \zeta(s) = v_0 + \frac{dF(w_0)}{dw} \zeta(s). \quad (61)$$

The particle displacements $s(t)$ are given by

$$\frac{ds(t)}{dt} = v_s[s(t)] = v_0 + \frac{dF(w_0)}{dw} \zeta(s). \quad (62)$$

The latter can be approximated by

$$\frac{ds(t)}{dt} = v_0 + \frac{dF(w_0)}{dw} \zeta(s) = v_0 + \frac{dF(w_0)}{dw} \zeta(v_0 t), \quad (63)$$

where we have set $s(t) = v_0 t$ in $\zeta(s)$. Thus, we obtain by integration

$$s(t) = v_0 t + \frac{dF(w_0)}{dw} \zeta(s) = v_0 t + \frac{dF(w_0)}{dw} \int_0^t dt' \zeta(v_0 t') \quad (64)$$

The displacement mean and variance are thus

$$m(t) = v_0 t, \quad \kappa(t) = 4\gamma v_0^2 \left[\frac{dF(w_0)}{dw} \right]^2 \int_0^t dt_1 \int_0^{t_1} dt_2 \int_0^{t_1} dt_3 \int_0^{t_3} dt_4 \langle \xi(v_0 t_2) \xi(v_0 t_4) \rangle. \quad (65)$$

Using that $\langle \xi(v_0 t_2) \xi(v_0 t_4) \rangle = v_0^{-1} \delta(t_2 - t_4)$, we obtain for the displacement variance

$$\kappa(t) = 4\gamma v_0 \left[\frac{dF(w_0)}{dw} \right]^2 \int_0^t dt_1 \int_0^{t_1} dt_2 \int_0^{t_1} dt_3 = \frac{4}{3} \gamma v_0 \left[\frac{dF(w_0)}{dw} \right]^2 t^3. \quad (66)$$

This explains the $\kappa(t) \propto t^3$ scaling observed in Figure 5 for $t \ll \tau_v$.

References

- [1] E. E. Adams and L. W. Gelhar. Field study of dispersion in a heterogeneous aquifer 2. spatial moment analysis. *Water Resour. Res.*, 28:3293–3307, 1992.
- [2] K. Alim, S. Parsa, D. A. Weitz, and M. P. Brenner. Local pore size correlations determine flow distributions in porous media. *Phys. Rev. Lett.*, 119:144501, Oct 2017. doi: 10.1103/PhysRevLett.119.144501. URL <https://link.aps.org/doi/10.1103/PhysRevLett.119.144501>.
- [3] R. Benke and S. Painter. Modeling conservative tracer transport in fracture networks with a hybrid approach based on the boltzmann transport equation. *Water Resour. Res.*, 39:1324, 2003. doi: 10.1029/2003WR001966,.
- [4] B. Berkowitz. Characterizing flow and transport in fractured geological media: A review. *Adv. Water Resour.*, 25(8-12):861–884, 2002.
- [5] B. Berkowitz, A. Cortis, M. Dentz, and H. Scher. Modeling non-fickian transport in geological formations as a continuous time random walk. *Rev. Geophys.*, 44:RG2003, 2006.
- [6] B. Bijeljic, P. Mostaghimi, and M. J. Blunt. Signature of non-Fickian solute transport in complex heterogeneous porous media. 107:204502, 2011.
- [7] P. Collon, D. Bernasconi, C. Vuilleumier, and P. Renard. Statistical metrics for the characterization of karst network geometry and topology. *Geomorphology*, 283:122–142, 2017.
- [8] A. Comolli, V. Hakoun, and M. Dentz. Mechanisms, upscaling and prediction of anomalous dispersion in heterogeneous porous media. *Water Resour. Res.*, accepted, 2019.
- [9] V. Cvetkovic, H. Cheng, and X.-H. Wen. Analysis of nonlinear effects on tracer migration in heterogeneous aquifers using Lagrangian travel time statistics. *Water Resour. Res.*, 32(6):1671–1680, 1996.
- [10] G. Dagan. Solute transport in heterogenous porous formations. *J. Fluid Mech.*, 145: 151–177, 1984.
- [11] G. Dagan. *Flow and transport in porous formations*. Springer, New York, 1989.
- [12] G. Dagan. Dispersion of a passive scalar in non-ergodic transport. *J. Fluid Mech.*, 233: 197–210, 1991.
- [13] P. de Anna, T. Le Borgne, M. Dentz, A. M. Tartakovsky, D. Bolster, and P. Davy. Flow intermittency, dispersion and correlated continuous time random walks in porous media. *Phys. Rev. Lett.*, 110:184502, 2013.
- [14] P. De Anna, B. Quaipe, G. Biroso, and R. Juanes. Prediction of velocity distribution from pore structure in simple porous media. *Phys. Rev. Fluids*, 2:124103, 2017. doi: 10.1103/PhysRevFluids.2.124103.
- [15] M. Dentz and J. D. Hyman. The hidden structure of hydrodynamic transport in random fracture networks. *Journal of Fluid Mechanics*, 977:A38, 2023.
- [16] M. Dentz, P. Kang, A. Comolli, T. Le Borgne, and D. R. Lester. Continuous time random walks for the evolution of lagrangian velocities. *Phys. Rev. Fluids*, 1(7):074004, 2016.

- [17] M. Dentz, P. K. Kang, A. Comolli, T. Le Borgne, and D. R. Lester. Continuous time random walks for the evolution of lagrangian velocities. *Physical Review Fluids*, 1(7): 074004, 2016.
- [18] M. Dentz, M. Icardi, and J. J. Hidalgo. Mechanisms of dispersion in a porous medium. *Journal of Fluid Mechanics*, 841:851–882, mar 2018. doi: 10.1017/jfm.2018.120.
- [19] J. L. Doob. The brownian movement and stochastic equations. *Annals of Mathematics*, pages 351–369, 1942.
- [20] A. Fiori, I. Jankovic, G. Dagan, and V. Cvetkovic. Ergodic transport through aquifers of non-gaussian log conductivity distribution and occurrence of anomalous behavior. *Water Resour. Res.*, 43:W09407, 2007.
- [21] A. Frampton and V. Cvetkovic. Significance of injection modes and heterogeneity on spatial and temporal dispersion of advecting particles in two-dimensional discrete fracture networks. 32(5):649–658, 2009.
- [22] L. W. Gelhar. *Stochastic subsurface hydrology*. Prentice Hall, 1993.
- [23] L. W. Gelhar and C. L. Axness. Three-dimensional stochastic analysis of macrodispersion in aquifers. *Water Resour. Res.*, 19(1):161–180, 1983.
- [24] L. W. Gelhar, C. Welty, and K. R. Rehfeldt. A critical review of data on field-scale dispersion in aquifers. *Water Resour. Res.*, 28(7):1955–1974, 1992.
- [25] N. Goeppert, N. Goldscheider, and B. Berkowitz. Experimental and modeling evidence of kilometer-scale anomalous tracer transport in an alpine karst aquifer. *Water research*, 178:115755, 2020.
- [26] V. Hakoun, A. Comolli, and M. Dentz. Upscaling and prediction of lagrangian velocity dynamics in heterogeneous porous media. *Water Resour. Res.*, 55:10.1029/2018WR023810, 2019.
- [27] M. Holzner, V. L. Morales, M. Willmann, and M. Dentz. Intermittent lagrangian velocities and accelerations in three-dimensional porous medium flow. *Phys. Rev. E*, 92: 013015, 2015.
- [28] J. D. Hyman and M. Dentz. Transport upscaling under flow heterogeneity and matrix-diffusion in three-dimensional discrete fracture networks. *Advances in Water Resources*, 155:103994, 2021.
- [29] J. D. Hyman, S. L. Painter, H. Viswanathan, N. Makedonska, and S. Karra. Influence of injection mode on transport properties in kilometer-scale three-dimensional discrete fracture networks. 2015.
- [30] J. D. Hyman, G. Aldrich, H. Viswanathan, N. Makedonska, and S. Karra. Fracture size and transmissivity correlations: Implications for transport simulations in sparse three-dimensional discrete fracture networks following a truncated power law distribution of fracture size. *Water Resour. Res.*, 52(8):6472–6489, 2016. ISSN 1944-7973. doi: 10.1002/2016WR018806. URL <http://dx.doi.org/10.1002/2016WR018806>.
- [31] P. K. Kang, M. Dentz, T. Le Borgne, and R. Juanes. Spatial markov model of anomalous transport through random lattice networks. *Phys. Rev. Lett.*, 107:180602, 2011.

- [32] P. K. Kang, J. D. Hyman, W. S. Han, and M. Dentz. Anomalous transport in three-dimensional discrete fracture networks: Interplay between aperture heterogeneity and injection modes. *Water Resources Research*, 56(11):e2020WR027378, 2020.
- [33] T. Le Borgne, M. Dentz, and J. Carrera. Spatial markov processes for modeling lagrangian particle dynamics in heterogeneous porous media. *Phys. Rev. E*, 78:041110, 2008.
- [34] M. Levy and B. Berkowitz. Measurement and analysis of non-fickian dispersion in heterogeneous porous media. *Journal of Contaminant Hydrology*, 64(3-4):203–226, 2003.
- [35] A. Massoudieh, M. Dentz, and J. Alikhani. A spatial markov model for the evolution of the joint distribution of groundwater age, arrival time, and velocity in heterogeneous media. *Water Resources Research*, 53(7):5495–5515, 2017.
- [36] V. L. Morales, M. Dentz, M. Willmann, and M. Holzner. Stochastic dynamics of intermittent pore-scale particle motion in three-dimensional porous media: Experiments and theory. *Geophysical Research Letters*, 44(18):9361–9371, 2017.
- [37] R. B. Nelsen. *An Introduction to Copulas*, volume 139. Springer Science & Business Media, 2013. ISBN 1475730764.
- [38] B. Noetinger, D. Roubinet, A. Russian, T. Le Borgne, F. Delay, M. Dentz, J.-R. De Dreuzy, and P. Gouze. Random walk methods for modeling hydrodynamic transport in porous and fractured media from pore to reservoir scale. *Transport in Porous Media*, pages 1–41, 2016.
- [39] S. L. Painter, V. Cvetkovic, and O. Pensado. Time-domain random-walk algorithms for simulating radionuclide transport in fractured porous rock. *Nuclear Technology*, 163(1): 129–136, 2008.
- [40] A. Puyguiraud, P. Gouze, and M. Dentz. Upscaling of anomalous pore-scale dispersion. *Transport in Porous Media*, 128(2):837–855, Apr. 2019. doi: 10.1007/s11242-019-01273-3. URL <https://doi.org/10.1007/s11242-019-01273-3>.
- [41] A. Puyguiraud, P. Gouze, and M. Dentz. Stochastic dynamics of lagrangian pore-scale velocities in three-dimensional porous media. *Water Resources Research*, 55(2): 1196–1217, Feb. 2019. doi: 10.1029/2018wr023702. URL <https://doi.org/10.1029/2018wr023702>.
- [42] Y. Rubin. *Applied stochastic hydrogeology*. Oxford University Press, New York, 2003.
- [43] P. Saffman. A theory of dispersion in a porous medium. *Journal of Fluid Mechanics*, 6(03):321–349, 1959.
- [44] T. Sherman, N. B. Engdahl, G. Porta, and D. Bolster. A review of spatial markov models for predicting pre-asymptotic and anomalous transport in porous and fractured media. *Journal of Contaminant Hydrology*, 236:103734, 2021.
- [45] M. Shlesinger. Asymptotic solutions of continuous-time random walks. *J. Stat. Phys.*, 10(5):421–434, 1974.
- [46] C. Syros. The linear boltzmann equation properties and solutions. *Physics Reports*, 45(4):211–300, 1978.
- [47] M. Williams. Radionuclide transport in fractured rock a new model: application and discussion. *Annals of Nuclear Energy*, 20(4):279–297, 1993.